ARTICLE NO. 80-4103

C 80-127

Linear Analysis of Poststall Gyrations

00001
00017

Mark A. Hreha* and Frederick H. Lutze†
Virginia Polytechnic Institute and State University, Blacksburg, Va.

The poststall gyrations of a high-performance aircraft are investigated by approximating the equations of motion with a linear mathematical model. Equilibrium poststall spin conditions are determined, which are not limited to small angles or spin rates and are used as reference conditions about which the linear model is developed. As a result, complete coupling between lateral and longitudinal motions is retained. Three aerodynamic models are evaluated using this linear analysis. These models include pure rotary derivatives obtained from VPI&SU stability tunnel, forced-oscillation data obtained from NASA tests, and a combination of the two which separates the unsteady and pure rotary derivatives. Results indicate that this last model gives better predictions of aircraft motion during poststall gyrations at high angles of attack and large sideslip angles. Comparisons are made with full-scale flight test results.

Nomenclature‡

b = wing span, m (ft)
$\bar{c}$ = mean aerodynamic chord, m (ft)
C_D = drag coefficient, $D/\bar{q}S$
C_L = lift coefficient, $L/\bar{q}S$
C_l = rolling moment coefficient, $L/\bar{q}Sb$
C_m = pitching moment coefficient, $M/\bar{q}S\bar{c}$
C_n = yawing moment coefficient, $N/\bar{q}Sb$
C_Y = side force coefficient, $Y/\bar{q}S$
D = drag force, $N(\text{lb}_\text{f})$
I_x = moment of inertia about x axis, kg-m^2 (slug-ft^2)
I_y = moment of inertia about y axis, kg-m^2 (slug-ft^2)
I_z = moment of inertia about z axis, kg-m^2 (slug-ft^2)
I_{xz} = product of inertia wrt x and z axes, kg-m^2 (slug-ft^2)
$L, (l)$ = lift force, N (lb), rolling moment m-N (ft-lb), (roll coefficient)
m = aircraft mass, kg (slug)
M = pitching moment, m-N (ft-lb)
N = yawing moment, m-N (ft-lb)
p = roll rate, rad/s
$\hat{p}$ = $pb/2V$
q = pitch rate, rad/s
$\hat{q}$ = $q\bar{c}/2V$
$\bar{q}$ = dynamic pressure, N/m^2 (lb/ft^2)
r = yaw rate, rad/s
$\hat{r}$ = $rb/2V$
S = wing (planform) area, m^2 (ft^2)
u,v,w = components of resultant velocity V along x,y, and z body axes, respectively, m/s (ft/s)
V = freestream velocity, m/s (ft/s)
Y = side force, N (lb)
α = angle of attack, deg
β = angle of sideslip, deg
ϕ = Euler bank angle, deg
θ = Euler attitude angle between horizon and x axis, deg
ψ = Euler yaw angle, deg

Stability Derivatives

$$C_{i_\alpha} = \frac{\partial C_i}{\partial \alpha}, \qquad i = D,L,Y,l,m,n$$

$$C_{i_\beta} = \frac{\partial C_i}{\partial \beta}$$

$$C_{i_{\dot{\alpha}}} = \frac{\partial C_i}{\partial (\dot{\alpha}\bar{c}/2V)}$$

$$C_{i_{\dot{\beta}}} = \frac{\partial C_i}{\partial (\dot{\beta}b/2V)}$$

$$C_{n_{\beta\text{dyn}}} = C_{n_\beta} - (I_z/I_x)C_{l_\beta}\sin\alpha$$

$$C_{i_p} = \frac{\partial C_i}{\partial (pb/2V)}$$

$$C_{i_q} = \frac{\partial C_i}{\partial (q\bar{c}/2V)}$$

$$C_{i_r} = \frac{\partial C_i}{\partial (rb/2V)}$$

Received Sept. 4, 1979; revision received Jan. 10, 1980.

Index categories: Handling Qualities, Stability and Control; Aerodynamics.

*Research Assistant, Dept. of Aerospace and Ocean Engineering.
†Associate Professor, Dept. of Aerospace and Ocean Engineering.

‡The longitudinal and lateral aerodynamic characteristics presented in this paper are referred to the body-axis system. Forces and moments are reduced to standard coefficient form on the basis of aircraft geometric properties.

Introduction

THE operational environments of current high-performance aircraft include frequent excursions to the edges of the airplanes' maneuvering flight envelopes. It is in this high angle-of-attack flight regime that military aircraft of the fighter or attack variety must display their most outstanding performance to fulfill the mission for which they are designed. Flight experience in test and actual combat situations has shown that aircraft flown in this regime are often pushed beyond their limits of controllability. Resulting stall/spin accidents involving losses of airplanes and aircrews constitute alarming statistics.[1,2] In addition, recent designs of future fighter configurations are continuing the trend of requiring flight at extreme angles of attack. Thus the need for reliable theoretical prediction of stall/poststall/spin characteristics is confirmed. The present research proposes an analytical method based on wind-tunnel measured aerodynamics for calculating the flight motions associated with a specific region of the stall/spin regime—the poststall gyration.

Implicit in the development of a reliable prediction technique is the proper use of measured aerodynamics in an

appropriate math model. It is proposed in this paper to use a combination of static, forced oscillation, and rotary aerodynamic data in conjunction with a fully coupled set of linear equations of motion. This approach, modeled after that of Anglin, is shown in his Fig. 1.[3]

A more complete discussion of aerodynamic modeling, as related to poststall dynamics, is given in Refs. 3-5. Pertinent to this study are the forced oscillation data such as $C_{n_r} - C_{n_{\dot\beta}}\cos\alpha$, $C_{l_p} + C_{l_{\dot\beta}}\sin\alpha$, and $C_{m_q} + C_{m_{\dot\alpha}}$, obtained from yaw, roll, and pitch oscillation tests, respectively, and the pure rotary derivatives such as C_{n_r}, C_{m_q}, and C_{l_p} obtainable from the curved and rolling flow stability wind tunnel located at Virginia Tech.[6-9] Although Anglin[3] has shown the need for combined rotary and forced oscillation data for predicting steady spins, oscillatory developed spins, and continuous rotation spin entries, a considerable amount of uncertainty as to the proper usage of these aerodynamic data in predicting poststall gyrations, spin entry, and oscillatory spin motions has been expressed by researchers. Furthermore, rotary data at low angles of attack and/or high sideslip angles associated with these types of motion have not been available. Consequently, little theoretical work has been conducted to determine poststall gyration prediction techniques.

Pure rotary data in these angle-of-attack and sideslip ranges are obtainable from the Virginia Tech Stability Wind Tunnel and can be used to examine some of these problems. The objective of this study is to present an analytical procedure and to assess the adequacy of various aerodynamic modeling for investigating the poststall gyration region. The scope of this study is set forth in the following outline:

1) Utilization of pure rotary data obtained in the Virginia Tech Stability Wind Tunnel along with pure lateral acceleration derivatives as opposed to the combined derivatives yielded by force oscillation tests.

2) Prediction of poststall gyrations using standard eigenvalue-eigenvector analysis of the fully coupled linear equations of motion.

3) Comparison of predicted results to full-scale flight test results.

Method of Approach

In this study the flight regime of interest is for angles of attack between 30 and 45 deg. The lower limit insures a fully stalled aircraft, while the upper limit is the limit of aerodynamic data available. Sideslip limits due to the limits of the aerodynamic data are ±10 deg. Throughout this flight region, the complete nonlinear equations are used to find all equilibrium conditions which had nonzero negative yaw rates.[10] Subsequently, a set of fully coupled linearized equations of motion are evaluated at each of these equilibrium points and a complete eigenvalue-eigenvector analysis is carried out. From these results, characteristics of the motion are determined, such as time to half or double amplitude, period, phase relations, etc. Results are compared for different aerodynamic models. In addition, some results are compared with actual full-scale flight tests. Additional discussion of the aerodynamic data used, the method of obtaining the equilibrium positions, the linearization procedure, and the source of the flight data is presented below.

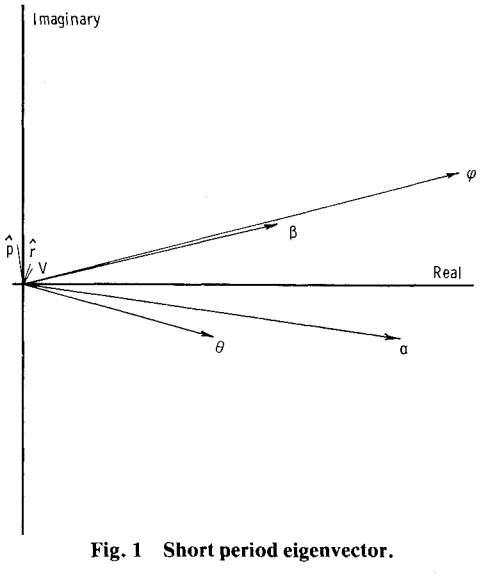

Fig. 1 Short period eigenvector.

Aerodynamic Data

The aerodynamic data come from two sources: stability wind-tunnel tests carried out at Virginia Polytechnic Institute and State University[6-9] and forced oscillation tests carried out at NASA Langley Research Center.[11] The subject aircraft of the present investigation is the twin-engine, single-place F-5 fighter. The NASA data and the VPI data were obtained with different model sizes and at slightly different dynamic pressures and Reynolds numbers. All lateral data used in the aerodynamic modeling were obtained from the VPI tests and treated as a function of angle of attack, sideslip, yaw rate, and roll rate as shown below, while longitudinal data were obtained from the NASA tests and treated as a function of angle of attack only.[11]

Briefly, the curved flow tests are conducted in a wind tunnel test section formed by deflecting the vertical walls of the nominally square section to the desired curvature. Wire screens of varying mesh sizes are positioned upstream of the test section to properly redistribute the velocity profile in the radial direction to be the same as that encountered in turning flight. The section provides curved airflow past the model allowing isolation of the pure yawing rotary stability derivatives. The pure rotary derivatives associated with rolling motion are obtained when the curved test section is replaced with the rolling flow section. For these tests, a motor-driven rotor device imparts a helical motion to the test section airstream creating solid vortex flow past the model. Thus the motion of an aircraft rolling about its velocity vector in still air is simulated. Further details are given in Refs. 6 and 7.

Aerodynamic data were constructed from the results of the rolling flow and curved flow wind-tunnel tests in the following manner. The rolling and yawing moment and side force coefficients were tabulated both as functions of α, β, and $\hat p$ and as functions of α, β, and $\hat r$, where $\hat p$ and $\hat r$ are nondimensional rolling and yawing rates. A linear combination of the lateral coefficients was formulated to model the influence of both rolling and yawing flow. A typical example for the rolling moment coefficient is:

$$C_l(\alpha,\beta,\hat p,\hat r) = C_{l_1}(\alpha,\beta,\hat r) + C_{l_2}(\alpha,\beta,\hat p) - C_{l_2}(\alpha,\beta,0)$$

where subscript 1 signals yawing flow data and subscript 2 denotes rolling flow data. The $\hat p = 0$ rolling flow influence is subtracted from the right-hand side of the preceding equation to avoid duplicating the static contribution from both sources of data. Note that all stability wind-tunnel data are taken in stability axes. The above calculations are performed in stability axes and converted to body axes to use in the analysis. The lateral data representations were incorporated with α-dependent longitudinal aerodynamics[11] and a three-dimensional interpolation scheme into a computer subprogram. The resulting aerodynamics generator is able to provide the six familiar force and moment coefficients for any given values of $\alpha,\beta,\hat p$, and $\hat r$. Complete details concerning the above developments are given in Ref. 10.

This aerodynamics package can be used to compute the static and dynamic stability derivatives in a procedure identical to numerical differentiation. To evaluate the yaw

Table 1 Equilibrium flight trajectories

	Aircraft geometry			Mass and inertia properties				
Equilibrium point	$\bar{c}$,m	b,m	S,m^2	m,kg	I_x,kg-m^2	I_y	I_z	I_{xz}
1	2.467	8.138	17.303	5882.20	4915	59290	62937	407
2,3	2.356	7.696	15.794	4553.30	2305	39997	40810	...

	Flight parameters							
Equilibrium point	α,deg	β,deg	V,m/s	θ,deg	ϕ,deg	$\dot{\psi}$,rad/s	$\bar{q}$,N/m^2	h,m
1	44.880	1.1282	111.545	−44.9210	−4.8829	−1.1214	2259	10,972
2	30.400	0.3310	149.047	−59.2000	−6.2400	−1.7700	3353	12,192
3	30.800	7.7600	147.828	−59.1000	8.1200	−1.7400	3298	12,192

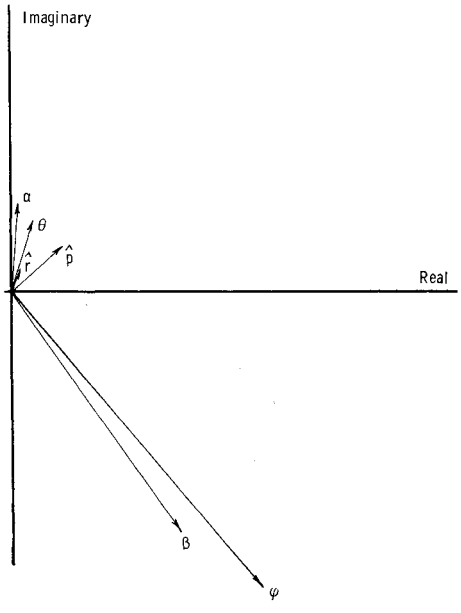

Fig. 2 Dutch Roll eigenvector.

rate derivatives for a specific flight condition, for example, the subroutine is entered with reference trajectory values of α,β, and $\hat{p}$, and a small difference from the nominal yawing rate $\hat{r}+\epsilon$. Upon return, the routine yields the coefficient values C'_Y, C'_l, and C'_N. A second entry with unchanged α,β, and $\hat{p}$ values, but yaw rate $\hat{r}-\epsilon$, produces the terms C''_Y, C''_l, and C''_N. The stability derivative C_{N_r} (damping in yaw) is then given by

$$C_{N_r}=\frac{\partial C_N}{\partial \hat{r}}\simeq\frac{\Delta C_N}{\Delta \hat{r}}=\frac{C'_N-C''_N}{\hat{r}+\epsilon-(\hat{r}-\epsilon)}=\frac{C'_N-C''_N}{2\epsilon}$$

which is, of course, evaluated at the nominal point $\alpha,\beta,\hat{p},\hat{r}$. Similar computations apply to the α,β, and $\hat{p}$ derivatives. Included in these calculations are the cross-coupling influences such as C_{l_α} (roll due to angle of attack). A list of the stability derivatives used in the linearized system is given in the Nomenclature.

The magnitude of the differencing parameter ϵ is determined by experimenting with nondimensional values in the range $0.1\geq\epsilon\geq0.0001$ and comparing the numerically computed derivatives with those indicated by the graphical aerodynamical data presented in Refs. 6 and 7 (e.g., C_l vs $\hat{r}$, C_N vs $\hat{r}$, etc.). Good correlation results with ϵ of the order 0.001 and subsequent calculations are made with this value.

Determination of Steady-State Equilibrium

Essential in the application of linear analysis to a specific problem is the existence of a nominal reference flight condition which characterizes the problem. This reference condition is an equilibrium point in the motion of a vehicle where both the angular and linear velocities of the body are constant. The equilibrium point is the solution vector of the general equations of motion with zero-time derivatives. Since a completely general analytic solution is impossible to obtain, the problem can be formulated in terms of optimization theory to extract the solution. This work has been accomplished by McCain.[10] The solution procedure involves minimization of a cost function defined as the sum of the squares of the state-time derivatives. The numerical optimization technique used is the Davidon-Fletcher-Powell (DFP) method which minimizes the specified cost function by a variation of the method of steepest descent. Reference 10 contains a detailed discussion of the procedure and its applications, as well as several references establishing the theoretical basis.

Implementing the DFP algorithm, McCain has determined four general areas of equilibrium points for the aircraft of concern in the present investigation. He has identified these areas as candidates for equilibrium spins on the basis that 1) the areas occur in the poststall angle-of-attack region, and 2) the aircraft's motion is described by descent in a helical path about a vertical axis. Correlation of the results of these equilibrium calculations with actual flight test data has shown that at least one of the areas characterizes (in the manner described below) a poststall gyration for this particular aircraft. Specifically, the present study is concerned with equilibriums in the angle-of-attack range of 30-45 deg combined with sustained yaw rates of about 60 deg/s. References 12 and 13 classify these motions as typical of poststall gyrations (psg). Therefore, it was possible to use several of the results cited in Ref. 10 as reference poststall conditions for the linear model. Additional equilibrium data were generated by implementing the DFP algorithm incorporating variations of the basic aircraft's mass and geometric properties. Some of these new equilibria were obtained for the properties of the aircraft for which full-scale flight test data were available (see Table 1).

Linearized Equations of Motion

The linearized model of the classical equations of motion has been used with enormous success in determining the dynamic stability characteristics of aircraft in steady rectilinear flight. This system governs the perturbations of the state vector about a nominal reference flight trajectory. On the other hand, some researchers have rejected linear analysis as unsuitable for spinning, poststall gyrations, or incipient spin applications where large variations may occur in the state variables, and aerodynamics are known to be highly nonlinear.[14] However, it has recently been suggested that valuable insight may be realized from an attempt to correlate spin entry with the stability or instability of the linearized equations.[15,16] Further, the application of linear theory to poststall angles of attack has led NASA researchers to important conclusions regarding aircraft directional divergence.[16] Haus[15] has applied the linear model to steady,

fully developed spins and has shown that the linearly predicted flight modes appear clearly in the nonlinear integrated solutions. With the restriction that linear analysis is applicable only to "short" time periods near the reference point, this research proposes that linear study of poststall gyrations may contribute to the understanding of the complex motions associated with this out-of-control flight regime and assess the importance of various aerodynamic models.

The classical equations of motion are linearized about an arbitrary equilibrium position which can include possible high angle of attack, large sideslip angle, and large roll, pitch, or yaw rate. The system contains the eight variables

$$X^T = [u, w, q, \theta, v, p, r, \phi]$$

which, upon completion of the linearization, are transformed into the conventional aircraft variables

$$X^T = [V, \alpha, q, \theta, \beta, p, r, \phi]$$

The aerodynamic forces and moments are assumed to be functions of all the motion variables with the longitudinal forces and moments being a function of the additional variable $\dot{w}$ ($\dot{\alpha}$), and the lateral forces and moments being a function of the additional variable $\dot{v}$ ($\dot{\beta}$), that is,

$$\text{longitudinal} \qquad f(u, v, w, p, q, r, \dot{w})$$

$$\text{lateral} \qquad f(u, v, w, p, q, r, \dot{v})$$

As a result, the linearized aerodynamic terms include several cross-stability derivatives relating longitudinal and lateral forces to lateral and longitudinal motions, respectively. A complete development of the linearized equations is presented in Appendix A of Ref. 17. It should be noted that the aerodynamic data were not sufficient to evaluate all of the derivatives in the linear model. Terms with insufficient data were set to zero.

Eigenvalue-Eigenvector Analysis

The linearization procedure outlined above leads to a set of eight first-order ordinary differential equations with constant coefficients. Associated with such a system is the so-called system matrix.[18] The roots of the characteristic equation associated with this matrix (characteristic determinant) are known as the eigenvalues. Corresponding to each eigenvalue is an eigenvector which represents the motion of the system associated with that eigenvalue. Each combination of eigenvalue and its eigenvector describes a characteristic or natural mode of motion. Due to the complexity and order of the system matrix, the eigenanalysis is performed numerically by standard computer routines.

In general, the eigenvalues are complex and appear in complex conjugate pairs $\lambda_{1,2} = n \pm i\omega$. The real part, n, determines the dynamic stability of the linear system. For $n > 0$ the amplitude of the motion increases exponentially in time and vice versa. Thus $n < 0$ corresponds to dynamic stability and $n > 0$ signals instability or divergence. The times to double or half of the initial values of state are given by

$$t_{\text{double/half}} = \frac{\ell n 2}{|n|}$$

Associated with the complex portion ω is the frequency of oscillatory motion or the period given by

$$T = \frac{2\pi}{\omega}$$

These parameters are descriptive measures of the characteristic modes and are used for convenient presentation of stability calculations in this paper.

The eigenvectors determine the relative values of the state variables in a natural mode. In each mode, all of the state variables change together in the same manner having identical frequencies and rates of growth or decay. Interpretation of the physics of any particular mode is facilitated by displaying the eigenvector in an Argand diagram.[18] This representation is used in the present paper to demonstrate the results. A typical diagram is given in Fig. 1.

Full-Scale Flight Tests

The flight test with which results are compared were obtained from a joint Air Force/Northrop Aircraft Division spin susceptibility program for the F-5E fighter aircraft. The test results, performance evaluations, and detailed description of the airplane are documented in Ref. 12. Geometric, mass, and inertial properties of the aircraft are presented as equilibrium point 1 in Table 1. Most of the flight histories documented pertain to aircraft configurations with the maneuver flap position selected. However, wind-tunnel data were available for the "clean" flaps-up configuration only. Consequently, direct numerical correlation of the linear analysis predictions could only be made for one case. The equilibrium point 1 in Tables 1-3 is compared with record A-18 in Ref. 12. The procedure for obtaining this comparison is discussed next.

The full-scale aircraft parameters are entered into the program used to find reference equilibrium points. Nominal equilibrium values near those obtained during the flight test are entered as a starting point and the program allowed to converge to an equilibrium condition. A linear analysis about this equilibrium is performed and the characteristics of the motion determined. The actual flight test data are scanned and sections with zero or constant control inputs isolated. The data for the longitudinal and lateral variables in these isolated sections are then examined and lines representing the mean values of the variables as well as the envelope curves constructed. From these, time to half or double amplitude, period, and component phasing are determined. By com-

Table 2 Dynamic stability derivatives

Model	Longitudinal Data		Lateral data								
					Rotary derivatives				Acceleration derivatives		
	C_{m_q}	$C_{m_{\dot{\alpha}}}$	C_{Y_p}	C_{l_p}	C_{n_p}	C_{Y_r}	C_{l_r}	C_{n_r}	$C_{Y_{\dot{\beta}}}$	$C_{l_{\dot{\beta}}}$	$C_{n_{\dot{\beta}}}$
1.1	−13.875	···	−1.5072	−0.1071	−0.5863	0.3223	0.0475	0.7485	···	···	···
1.2	−27.750	···	−4.2500	−0.2250	−0.9200	5.5000	0.2750	1.5500	···	···	···
1.3	−13.875	−13.875	−1.5072	−0.1071	−0.5863	0.3223	0.0475	0.7485	−4.9639	−0.1708	−1.4178
2.1	− 9.500	···	0.2309	0.1989	−0.3116	1.7203	−0.2050	−0.2234	···	···	···
2.2	−19.000	···	−0.3500	0.0800	−0.3000	2.0000	−0.2300	0.3400	···	···	···
2.3	− 9.500	− 9.500	0.2309	0.1989	−0.3116	1.7203	−0.2050	−0.2234	−0.7595	−0.0976	−0.4803
3.1	− 9.500	···	−0.7245	−0.1528	0.0646	1.8075	−0.0819	−0.0065	···	···	···
3.2	−19.000	···	−0.3500	0.0800	−0.3000	2.0000	−0.2300	0.3400	···	···	···
3.3	− 9.500	− 9.500	−0.7245	−0.1528	0.0646	1.8075	−0.0819	−0.0065	−0.7595	−0.0976	−0.4803

Table 3 Results of dynamic stability calculations

Model	Short period			Dutch Roll	Synchronous oscillation: Component phasing				Component phasing	
	T,s	$t_{1/2}$,s	T,s	$t_{1/2}$,s	p/β, deg	p/ϕ, deg	T,s	$t_{1/2}$, s	α/θ, deg	ϕ/θ, deg
1.1	3.213	0.571	1.624	−2.491[a]	93.864	88.959	5.574	7.970	0.369	88.956
1.2	3.351	0.533	1.610	−3.865	95.655	90.841	5.575	8.007	0.265	89.126
1.3	3.352	0.544	1.613	−3.227	96.983	92.156	5.576	7.991	0.335	88.991
A18[b]	3.300	2.400	1.600	−3.600	99.000	105.000	5.400	8.000	0.0	...
2.1	2.280	0.933	7.091	−0.235	17.156	17.393	3.544	10.723	−0.043[c]	89.410
2.2	2.318	0.760	5.307	−0.243	23.531	23.896	3.545	10.792	−0.137	89.504
2.3	2.315	0.828	6.021	−0.239	21.003	21.314	3.545	10.736	−0.079	89.443
3.1	2.386	1.268	1.100	2.474	95.373	93.070	3.604	10.564	0.631	89.277
3.2	2.493	1.274	1.088	−2.160	91.067	88.791	3.602	10.437	1.352	88.539
3.3	2.433	1.097	1.097	2.015	97.488	95.118	3.605	10.598	0.588	91.415

[a] Negative values of $t_{1/2}$ indicate instability. [b] Flight test, Ref. 12. [c] Negative values of α/θ indicate α lags θ.

paring these results with the linearized results, certain modes can be identified and detailed comparisons made, such as those in Table 3.

Results

An important objective of this research is to determine the effect of various aerodynamic models on the predicted motion for each of the reference conditions and, in addition, to compare predicted motions with full-scale flight data of Ref. 12 where possible. In order to accomplish this, the results of dynamic stability calculations using three types of aerodynamic models are compared. The three sets of data are: 1) the Virginia Tech Stability Wind Tunnel (VPI) data acquired and computed by the procedures specified in the Aerodynamic Data section. These data include pure rotary data and no unsteady aerodynamic data (e.g., C_{n_r}, etc.); 2) (NASA) forced oscillation data as reported in Ref. 11 with the combined data assigned to the pure rotary derivative terms (e.g., $C_{n_r} - C_{n_{\dot\beta}} \cos\alpha \rightarrow C_{n_r}$, etc.); and 3) combined VPI and NASA data (VPI-NASA) where the component derivatives of the force data are separated by subtracting the pure rotary derivatives (VPI) from the forced-oscillation data (NASA) to yield isolated acceleration derivatives to be used with the pure rotary derivatives (e.g., C_{n_r}, $C_{n_{\dot\beta}}$, etc.).

Comparison of the results obtained with data sets 1 and 3 allows the evaluation of the acceleration derivative influence since set 1 accounts only for pure rotary derivatives. Usage of the second data set (NASA) enables one to investigate the integrity of a widely used computational model which treats the forced-oscillation data as pure rotary derivatives. The final data set represents a new aerodynamic model which seems to yield different results in certain complex applications, such as those of interest here.

For purposes of representation, the dynamic stability input data given in Table 2 are identified by the notation E.*d* where E represents one of the three equilibrium points listed in Table 1 and *d* denotes the type of data, or aerodynamic model, used (i.e., $d=1$ for VPI data, $d=2$ for NASA data, and $d=3$ for VPI-NASA data). The results of the dynamic stability calculations are presented in Table 3.

Discussion of Results

For rectilinear trajectories, the phugoid, short-period longitudinal, and Dutch Roll lateral modes are well-known oscillatory motions associated with flight vehicles. In addition, two real roots corresponding to rolling convergence and spiral motions are usually present. These familiar modes of flight were clearly identified for the subject aircraft. Dynamic stability calculations were made for straight and level flight references with equilibrium angles of attack from 5 deg through stall (23 deg) up to poststall values of 40 deg. The

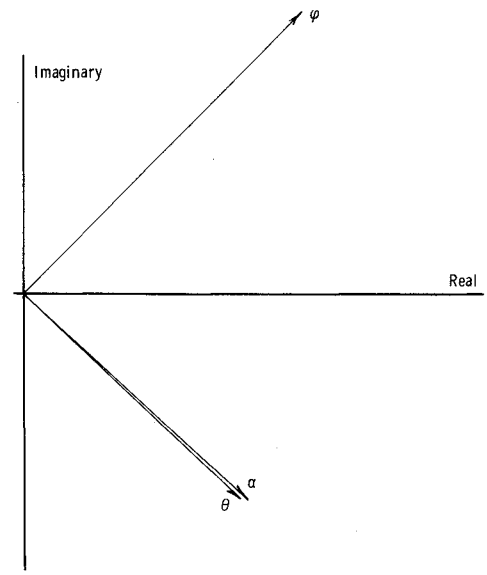

Fig. 3 Sychronous oscillation eigenvector.

5-30 deg angle-of-attack (AOA) equilibriums were generally characterized by stable oscillatory roots and convergent real roots. At a 31 deg angle of attack, the Dutch Roll mode became unstable and remained so throughout the poststall region. This onset of lateral instability suggests directional divergence near 31 deg, which corresponds well with full-scale performance evaluations. Pilots noted that attempts to control bank angle with aileron were ineffective because the airplane lateral motions were dominated by excessive nose slice and wing rock above 30 deg AOA.[12] Note that the $C_{n_{\beta dyn}}$ prediction parameter indicates no divergence at angles of attack through 40 deg for this airplane,[11] demonstrating that $C_{n_{\beta dyn}}$ is not reliable as a departure indicator.

When linearization was performed about equilibrium spin candidates having yaw rate about 60 deg/s and AOA in the range 40-50 deg, three oscillatory roots were identified along with two real roots (see, for example, equilibrium point 1, Table 1, and corresponding data in Tables 2 and 3). Clearly, one root is a continuation of the short-period longitudinal mode and another is the continuation of the Dutch Roll motion. The short-period eigenvector exhibits large lateral components in addition to the usual longitudinal components due to the inclusion of cross-coupling derivatives (e.g., C_{l_α}, C_{n_α}, etc.) in the linearized model and the complex nature of the equilibrium point. As shown in the Argand diagrma (Fig. 1), the short period is dominated by α,θ,ϕ components, the latter two almost in phase. This mode was always found to be stable and heavily damped.

Likewise, the Dutch Roll, which contains strictly lateral components in rectilinear flight, displays longitudinal components α and θ along with $\hat{p}$, ϕ, and β. For the poststall reference of interest here, the Dutch Roll mode was determined to be divergent with a period of the order of two seconds. The major components of the Dutch Roll eigenvector are the sideslip and roll attitude perturbations as shown in Fig. 2.

A third oscillatory mode and two nonoscillatory modes replace the longitudinal phugoid and the real roll and spiral roots. Haus[15] was first to identify this stable oscillatory root in the fully developed steady-spin equilibrium. He has termed the mode "synchronous oscillation," noting that the imaginary part ω of its eigenvalue yields the angular velocity of the spin associated with the equilibrium. The present research confirms that for each of the spin equilibrium conditions reported in Ref. 10 for the subject aircraft, the ω of the synchronous oscillation eigenvalue is the vehicle spin rate $\dot{\psi}$. No case of unstable synchronous oscillation was found for the airplane in a number of spin flight conditions which supports a similar conclusion stated by Haus. The mode is characterized by major components θ, α, and ϕ where θ and α are invariably in phase and lag ϕ by almost exactly 90 deg (see Fig. 3). The synchronous oscillation is a characteristic of the spinning motion.

The three modes previously discussed have short periods characterized, in many cases, by eigenvalues of the same order. As noted, for the complex motions associated with poststall flight trajectories, each mode consists of a mixture of longitudinal and lateral components. Although two of the modes have been given names suggesting rectilinear uncoupled motion, it is not possible to technically separate the longitudinal mode from the lateral. The two real eigenvalues also exhibited both lateral and longitudinal characteristics—one was stable, the other divergent. The times to half and double amplitude were about 4 and 0.5 s, respectively.

It should be emphasized here that all the poststall equilibrium conditions investigated had some unstable eigenvalues. Hence, these conditions do not represent possible steady-state spin situations since divergent motion away from them would occur. However, it is proposed that the motions, as displayed by the eigenvectors, would be typical of the poststall gyrations of the aircraft as it moves toward a new equilibrium condition which could be toward a normal flight condition at lower angle of attack or possibly to a stable equilibrium spin at a high angle of attack.

The results of the linear calculations presented in Table 3 are designed to 1) show correlation between predicted motions and motions observed during flight tests, and 2) evaluate the three different aerodynamic models referred to in the previous section. In order to verify that the linearized mathematical model is, indeed, a reliable dynamics predictor, it was necessary to compute reference flight trajectories corresponding to the time histories given in Ref. 12 using the reported aircraft geometric and mass parameters. Equilibrium point 1 (Table 1) represents the correct major characteristics of A18 such as α,β, and yaw rate. The linearly obtained characteristics (oscillation periods, times to decay or increase, and component phasing) for all aerodynamic models shows excellent correlation with flight test dynamics, except for the $t_{1/2}$ of the short period. This discrepancy is most likely due to a lack of proper representation for the longitudinal aerodynamic data. As noted in the description of the aerodynamic data, only α-dependent longitudinal data were available. It is noted that the trends suggested by other calculations were clearly revealed in the flight tests made with flaps deflected, although actual numerical values differed.

Comparison of the computation results of the VIP data (1.1) and VPI-NASA data (1.3) indicates that a model using only pure rotary derivatives yields basic trends of the dynamics, but the acceleration derivatives must be employed to more accurately simulate the stability characteristics of the Dutch Roll and short period. Aerodynamic model 1.2 (NASA data) is seen to be very consistent with the 1.3 model in its predicted results (see Table 3), indicating that equating forced-oscillation data to the pure rotary derivatives may be applicable in poststall analysis. The results of calculations concerning equilibrium points 2 and 3, however, do not substantiate this procedure.

Table 1 shows that the major differences in the flight parameters for equilibriums 2 and 3 occur in the state variables β (sideslip angle) and ϕ (roll attitude angle). Both reference trajectories are reported by McCain[10] as spin candidates. Neither trajectory has been detected in real-flight situations for this aircraft (at least no spins or spin entries are reported at $\alpha = 30$ deg in Ref. 12), although the equilibriums are mathematically possible and the characteristics presented in Table 1 do describe the motion of a spinning vehicle. The equilibrium points are, therefore, valid references to be used in the further evaluation of NASA and VPI-NASA aerodynamic models.

The results of Table 3 concerning models 2.1, 2.2, and 2.3 parallel the discussion just given for equilibrium point 1. However, an extremely important phenomenon is noted in the calculations with respect to equilibrium point 3. The 3.2 model (pure rotary derivatives equal to the forced-oscillation data) predicts instability in the Dutch Roll, while model 3.3 (separated acceleration and rotary derivatives) indicates a stable Dutch Roll. The models are in agreement for the other two modes. The discrepancy may arise from the large sideslip angle β, since the models are compatible for equilibrium 2 ($\beta = 0.331$ deg) and incompatible for equilibrium 3 ($\beta = 7.76$ deg). It should be noted that the bank angles of the two equilibrium conditions are quite different and, although the bank angle should not influence the aerodynamics, it does appear in the characteristic equation coefficients and can affect the eigenvalues. However, Haus[15] has verified that reduction of the linear system to sixth order by deletion of the θ and ϕ governing equations has little effect on the short-period and Dutch Roll characteristics. The difference in ϕ between equilibriums 2 and 3 apparently should not be of concern in the present discussion.

The results imply that the model, which assigns the value of the forced-oscillation data to the pure rotary derivatives, cannot account for the effect of large sideslips. Only the dependence of angle of attack is expressed in the dynamic data. It is not surprising then that this model yields good results for equilibriums 1 and 2 where the sideslip angles are very small. On the other hand, as explained previously, the VPI data, determined through rolling and curved flow wind-tunnel tests, incorporates not only the dependence of lateral aerodynamics on α but also on β, roll rate, and yaw rate. This dependence must be considered in selecting an aerodynamic model for oscillatory spin and poststall analysis; sideslips and angular velocities are known to be excessive in these flight regions. As stated previously, equilibrium points 2 and 3 have not been established as real poststall spins, but at least one flight test history of similar reference conditions (as point 3 but with flaps deflected) indicates that the Dutch Roll is stable for this angle-of-attack and sideslip combination (see for example, History A23, Ref. 12).

Conclusions

A very detailed linearization of the general equations of motion has been performed; no small-angle assumptions have been made and complete coupling between the lateral and longitudinal motions retained. The linear system is used to investigate the complex dynamics associated with poststall gyrations and to evaluate several aerodynamic models proposed for the computation of these motions. Selected results are presented which support the following conclusions:

1) The linear analysis appears as a viable approach to

predict poststall gyrations based solely on wind-tunnel-obtained aerodynamic data. For the single flight test record reported here, the results were good.

2) For the subject aircraft, three oscillatory motions were identified in the poststall region—coupled short period, unstable Dutch Roll, and the synchronous oscillation mode. These motions clearly exist in the full-scale flight test histories, although only one could be directly compared here.

3) For the case where the reference poststall conditions have small sideslip angles, all the aerodynamic models do equally well in predicting the characteristic motions.

4) A new aerodynamic model is proposed which incorporates the effects of α,β, roll, and yaw rate in the pure rotary derivatives and also allows separation of the acceleration derivatives from combined oscillation data. This model yields substantially different results for the case where large sideslip angles are involved.

Acknowledgment

This work was partially supported by NASA Langley Research Center under Contract NASI-13175, Task Authorization No. 16.

References

[1] Sewell, C.A. and Whipple, R.D., "F-14A Stall and Spin Prevention System Flight Tests," *Stall/Spin Problems of Military Aircraft,* AGARD-CP-199, 1976.

[2] Money, A. F. and House, D.E., "U.S. Navy Flight Test Evaluation and Operational Experiences at High Angle of Attack," *Stall/Spin Problems of Military Aircraft,* AGARD-CP-199, 1976.

[3] Anglin, E.L., "Aerodynamic Characteristics of Fighter Configurations During Spin Entries and Developed Spins," *Journal of Aircraft,* Vol. 15, Nov. 1978. pp. 769-776.

[4] Chambers, J. R., Bowman, J.S., and Malcolm, G.N., "Stall/Spin Test Techniques Used by NASA," *Stall/Spin Problems of Military Aircraft,* AGARD-CP-199, 1976.

[5] Malcolm, G.N., "New Rotation-Balance Apparatus for Measuring Airplane Spin Aerodynamics in the Wind Tunnel," *Journal of Aircraft,* Vol. 16, April 1979, pp. 264-268.

[6] Lutze, F.H., Jr., "Curved Flow Wind Tunnel Test of a Spin-Resistant Aircraft Configuration," Virginia Polytechnic Institute and State University, VPI-Aero-067, Aug. 1977.

[7] Lutze, F.H., Jr., "Rolling Flow Wind Tunnel Test of a Spin-Resistant Aircraft Configuration," Virginia Polytechnic Institute and State University, VPI-Aero-075, Dec. 1977.

[8] Lutze, F.H. and Cliff, E.M., "New Calibration on Corrections for the VPI&SU Stability Wind Tunnel Curved Flow Test Section," Virginia Polytechnic Institute and State University, VPI-Aero-069, Aug. 1977.

[9] Lutze, F.H., Jr., "Calibration of the VPI&SU Stability Wind Tunnel Rolling Flow Test Section," Virginia Polytechnic Institute and State University, VPI-Aero-070, Aug. 1977.

[10] McCain, C.E. Jr., "Utilization of Aerodynamic Coefficients Generated by Pure Rolling and Pure Yawing Flow in the Determination of Aircraft Equilibrium Spin Properties," Masters Thesis, Virginia Polytechnic Institute and State University, June 1978.

[11] Grafton, S.B., Chambers, J.R., and Coe, P.L., Jr., "Wind-Tunnel Free-Flight Investigation of a Model of a Spin-Resistant Fighter Configuration," NASA TN D-7716, June 1974.

[12] Arent, L.E., Wilson, D.B., and Taylor, J.H., "F-5E Stall/Post-Stall/Spin Susceptibility Test," AFFTC-TR-76-30, Oct. 1976.

[13] Taylor, J.H., "F-5E Spin Susceptibility Test," The Society of Experimental Test Pilots 1976 Report, *XX Symposium Proceedings,* Tech. Review Vol. 13, No. 1-2, Sept. 1976, pp. 43-50.

[14] Woodcock, R.J. and Weissman, R., "The Stall/Spin Problem" *Stall/Spin Problems of Military Aircraft,* AGARD-CP-199, 1976.

[15] Haus, F.C., "Stability of Helicoidal Motions at High Incidences," *Stall/Spin Problems of Military Aircraft,* AGARD-CP-199, 1976.

[16] Chambers, J.R. and Anglin, E.L., "Analysis of Lateral-Directional Stability Characteristics of a Twin-Jet Fighter Airplane at High Angles of Attack," NASA TN D-5361, June 1969.

[17] Hreha, M.A., "Linear Analysis of Incipient Spin Dynamics," Masters Thesis, Dept. of Aerospace and Ocean Engineering, Virginia Polytechnic Institute and State University, June 1979.

[18] Etkin, B., *Dynamics of Atmospheric Flight,* Wiley, New York, 1972.